

ESTIMATION OF PARTICLE SIZE BASED ON LDV
MEASUREMENTS IN A DE-ACCELERATING FLOW FIELD

James F. Meyers
NASA Langley Research Center
Hampton, Virginia

PARTICLE SIZE CONSIDERATIONS

The accuracy of velocity measurements made with a laser velocimeter is strongly dependent upon the response of the seeding particles to the dynamics of the flow field. The smaller the particle the better the response to flow fluctuations and gradients and therefore the more accurate velocity measurement. In direct conflict is the requirement of light scattering efficiency to obtain signals with the laser velocimeter which, in general, is better as the particle size is increased. In low speed flow fields these two requirements on particle size overlap and accurate measurements may be obtained. However in high speed flows, where the velocity gradients may be severe, very small particles are required to maintain sufficient dynamic response characteristics to follow the flow. Therefore if velocity measurements are to be made in these flows, the laser velocimeter must be designed with sufficient sensitivity to obtain signals from these small particles. The present paper describes an insitu determination of the size distribution of kaolin particles ($\text{Al}_2\text{O}_3 \cdot 2 \text{SiO}_2 \cdot 2 \text{H}_2\text{O}$) in the 16-foot Transonic Tunnel and the sensitivity characteristics of the laser velocimeter system.

SMALL ENOUGH TO FOLLOW THE FLOW FIELD

- SIZE
- SHAPE
- DENSITY

LARGE ENOUGH FOR THE LV TO "SEE" IT

- SIZE
- SHAPE
- INDEX OF REFRACTION

APPLICATION CONSIDERATIONS

The choice of seeding material for laser velocimetry applications is limited to using particles naturally present in the flow, or injecting either liquid droplets or solid particles in the flow. Natural particulates have the advantage of not requiring a seeding generation system and no additional facility contamination; however, they are of unknown size and are very few in number. This leads to unknown measurement accuracies and long test times. Liquid seeding, especially liquids with relatively high vapor pressures, has the advantage of yielding large numbers of particles while maintaining little facility contamination because they will evaporate. Liquids, however, usually have fairly wide size distributions which are typically skewed toward the larger sizes. These distributions may also be modified by the test conditions within the facility. Solid particles have the advantage of yielding large numbers of particles while maintaining their size distributions. Solid particles may present a contamination problem, may have higher densities than liquid particles (which affects particle dynamics), and may erode the model/tunnel surfaces.

NATURAL PARTICULATES

- SIZE UNKNOWN
- LOW DATA RATE

LIQUID SEEDING

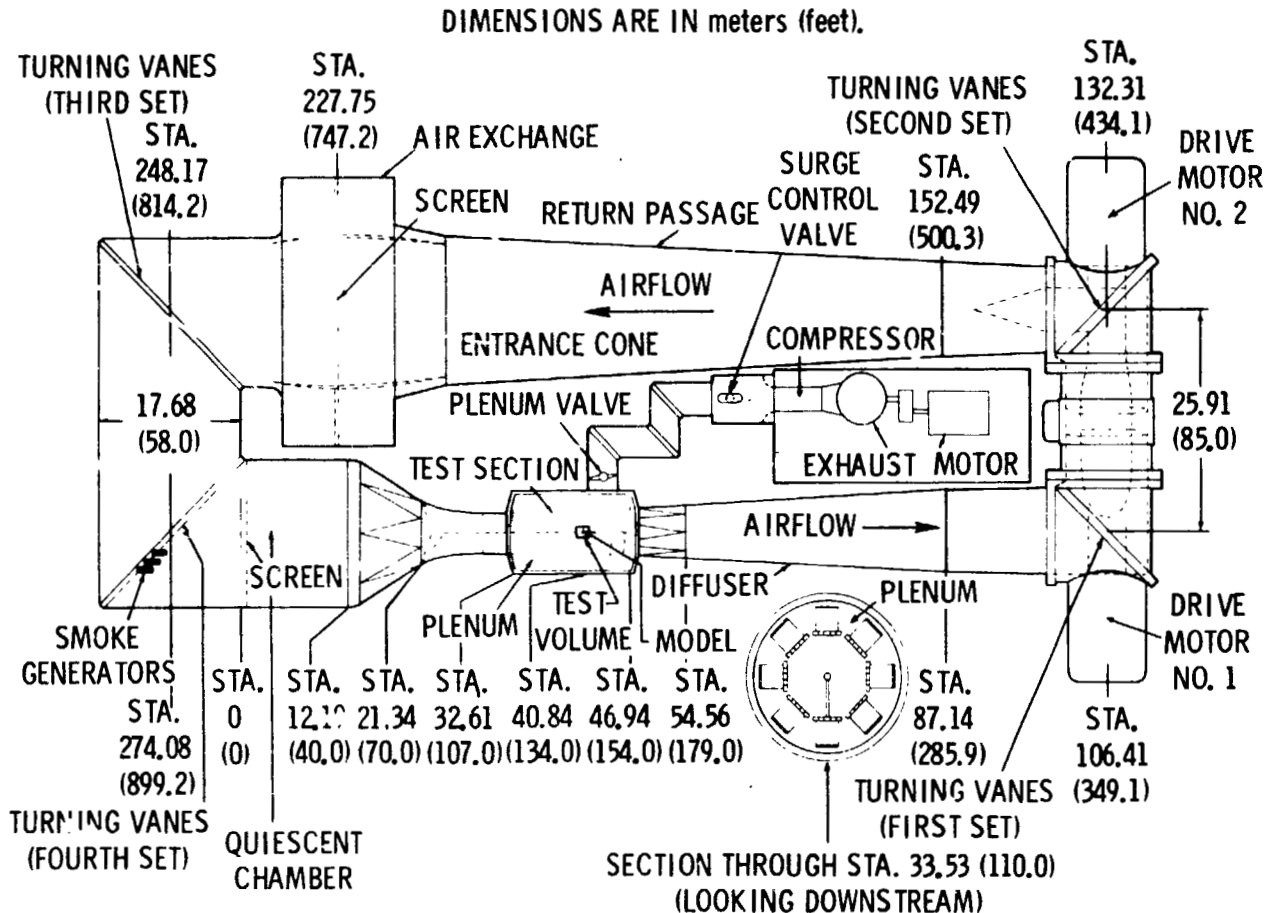
- SIZE DISTRIBUTION SKEWED
- MODIFICATION BY TEST CONDITIONS

SOLID PARTICULATES

- SIZE DISTRIBUTION
- DENSITY
- MODEL EROSION

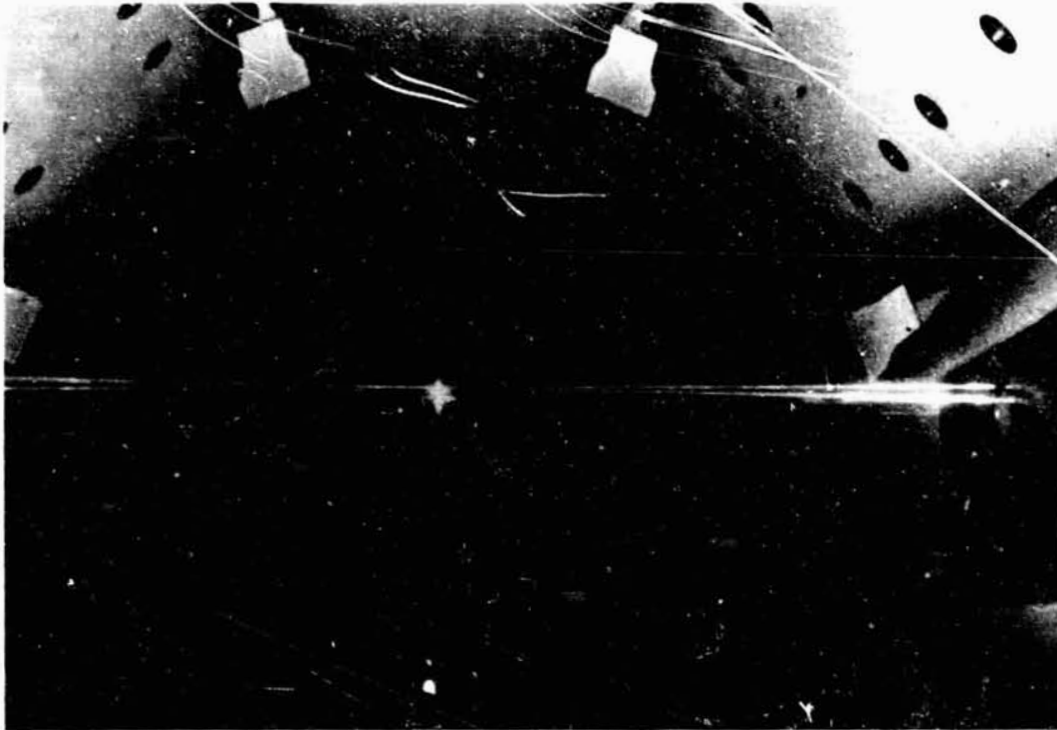
ARRANGEMENT OF THE LANGLEY 16-FOOT TRANSONIC TUNNEL

The figure illustrates the layout of the 16-foot transonic tunnel along with the location of the particle generation system. It is noted that only three generators are illustrated while the actual system contained ten. The laser velocimeter system is located within the plenum chamber surrounding the test section. The wind tunnel has a Mach number range up to 1.3 and an average Reynolds number of 13×10^6 per meter at Mach numbers above 0.6. The test section is octagonal with movable walls used to minimize the axial Mach number gradient and is slotted for removal of the boundary layer by evacuation of the surrounding 9.75 meter diameter plenum at Mach numbers above 1.03. The ambient conditions within the plenum chamber at Mach 1.0 are approximately 0.5 atm pressure, 50° C and 150 dBm of acoustic power. The structural members within the plenum chamber are subjected to vibration levels of up to 5 g. Optical access to the test section from the plenum is provided by an optical quality (BK-7 glass) window installed in the test section wall with a clear viewing area of 1.27 m by 0.91 m.



HEMISPHERE-CYLINDER MODEL INSTALLED IN THE TEST SECTION

The sting mounted hemisphere-cylinder model is shown in the figure located along the centerline of the 16-foot transonic tunnel test section. The laser beams from the laser velocimeter located in the plenum chamber are shown passing in front of the model.



ORIGINAL PAGE IS
OF POOR QUALITY

HEMISPHERE-CYLINDER MODEL

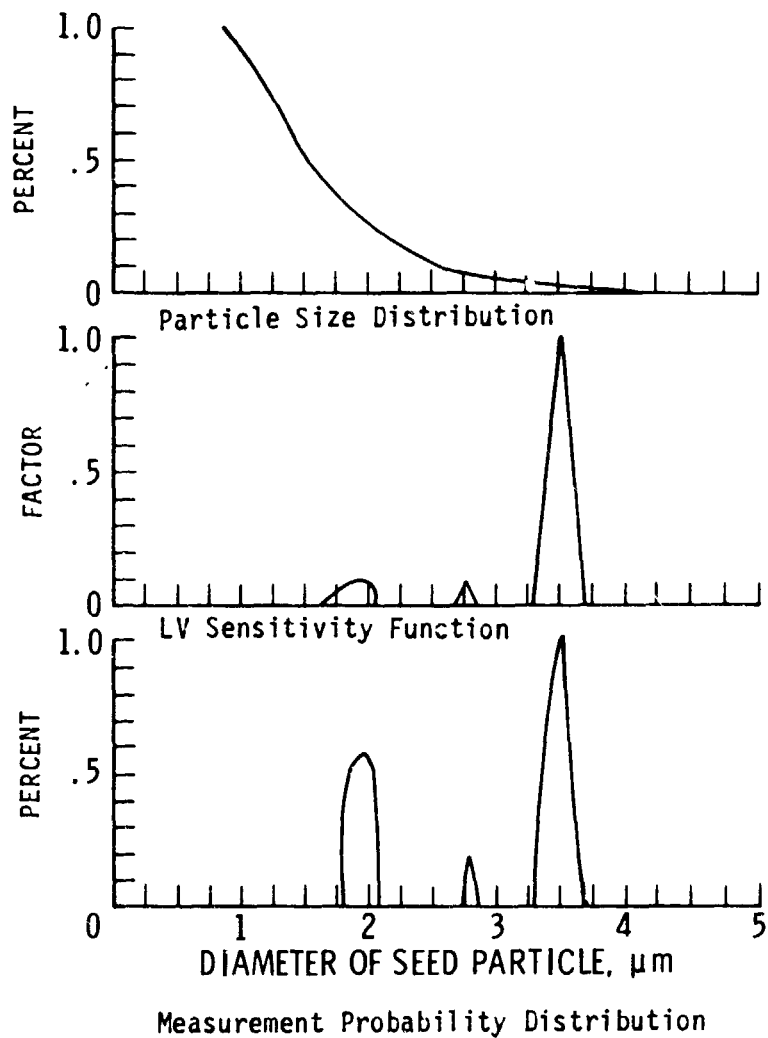
The hemisphere-cylinder model along with the laser beams is shown in the figure. The hemisphere is 19.05 cm in diameter followed by a 10.16 cm long cylinder.



OPTICAL PARTICLE SIZE ANALYSIS - KEROSENE

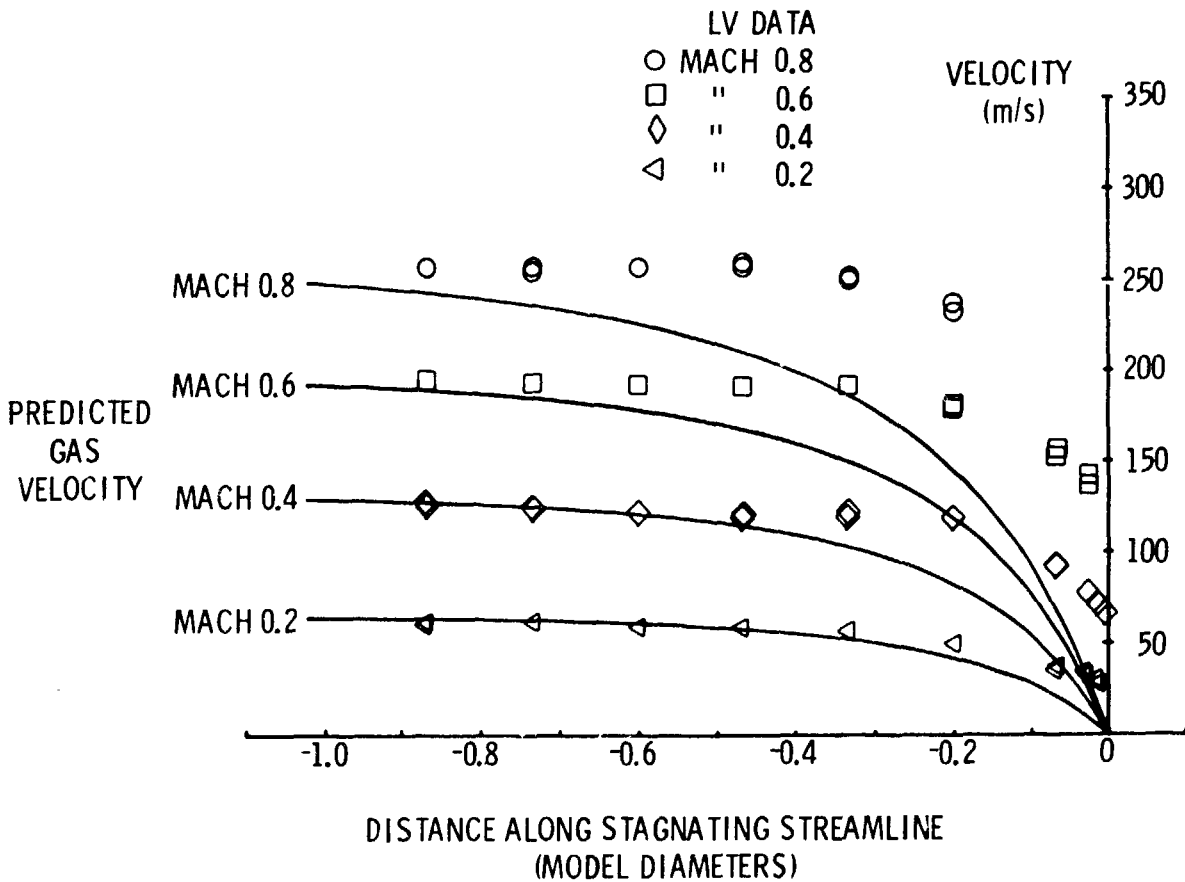
The first test of the laser velocimeter in the 16-foot transonic tunnel used kerosene as the seeding material. The particle size distribution of kerosene, the theoretical sensitivity function for the proof-of-concept laser velocimeter calculated using the simulation code described in reference 1, and the resulting detectable particle size distribution are illustrated in the figure. The measured particle size distribution was obtained in the laboratory using an optical particle size analyzer with the particle generator located a distance from the analyzer to yield a corresponding time-of-flight as in the tunnel to simulate the effects of evaporation.

The calculation of the theoretical sensitivity function begins with the determination of the electro-magnetic field resulting from the scatter of light from a particle of a given size (described by Mie in reference 2) as it passes through each pair of the laser beams comprising the sample volume. The interaction between the two scattered fields is calculated over the collecting solid angle of the laser velocimeter using the method described in reference 3 to yield the optical transfer function which is used along with the Gaussian intensity profile of the laser beams to obtain the theoretical signal burst. This burst is integrated and used to drive a Poisson random number generator yielding a Monte Carlo simulation of photon arrivals at the photocathode surface of the photomultiplier. The photons are convolved with the photomultiplier transfer function to obtain the electronic signal burst which is then input to a model of a high-speed burst counter with double threshold detection circuits and a 5:8 count comparison to determine if the signal has sufficient amplitude to yield a velocity measurement. If the signal does not have sufficient amplitude, following band pass filtering, for ten consecutive cycles to cross the thresholds with sufficient signal-to-noise ratio to satisfy the 5:8 count comparison test, a measurement can not be made and the sensitivity factor is zero for that particle size. If the signal is accepted by the counter, the amplitude of the signal is reduced in an exponential manner until the signal fails to be accepted by the counter. The amount of reduction in amplitude corresponds to a distance from the center of the sample volume in accordance with the Gaussian intensity profile of the laser beams. A sensitivity factor of unity is assigned where the distance from the center of the sample volume corresponds to the sample volume radius as defined by the intensity being $1/e^2$ of the intensity at the center. The resulting sensitivity function is then multiplied by the measured particle size distribution to yield the distribution of detectable particles.



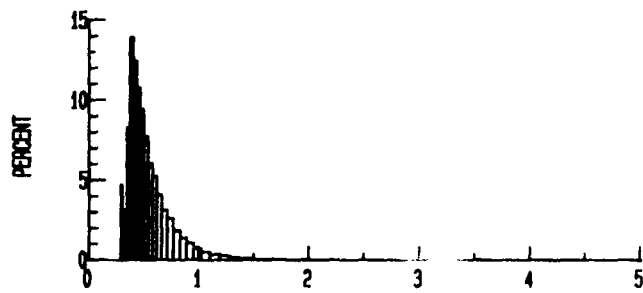
LV MEASUREMENTS ALONG THE STAGNATING STREAMLINE

Velocity measurements were made along the stagnating streamline from one model diameter upstream to within an estimated distance of 1.9 mm from the model surface for several Mach numbers. These measurements along with the predicted gas velocity profiles using the potential flow method outlined in reference 4 are illustrated in the figure. The size of the kerosene particles which would yield the velocities measured by the laser velocimeter was determined using the particle dynamic prediction procedures outlined in reference 5. The resulting particle size was found to be in excess of 17 micrometers which indicates that the particle size distribution was modified by the conditions within the tunnel. Therefore kerosene has been shown to be a very poor choice as the seeding material for the 16-foot transonic tunnel.

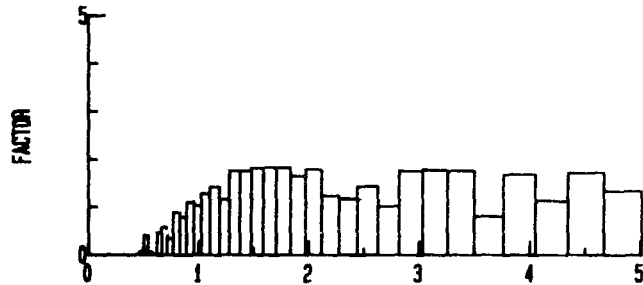


AERODYNAMIC PARTICLE SIZE ANALYSIS - KAOLIN

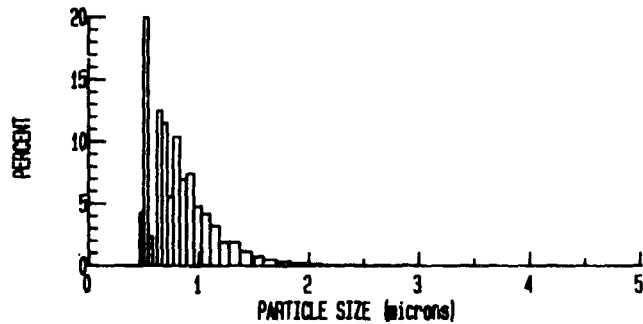
Kaolin was chosen as the next particle material. Kaolin particles are irregular in shape with a specific gravity of 2.58 and an index of refraction of 1.56. The particles were suspended in ethanol and injected into the tunnel using the same particle generators. Within a short distance from the generators, the ethanol evaporated leaving the kaolin particles embedded in the flow field. The measurement of the particle size distribution in the laboratory was performed using an aerodynamic particle size analyzer which yielded an equivalent spherical size distribution of the irregularly shaped kaolin. This size distribution was then used to determine the sensitivity function and the resulting detectable particle size distribution. These results, illustrated in the figure, indicate that the average detectable particle was 0.78 micrometers in diameter.



a) Particle Size Distribution



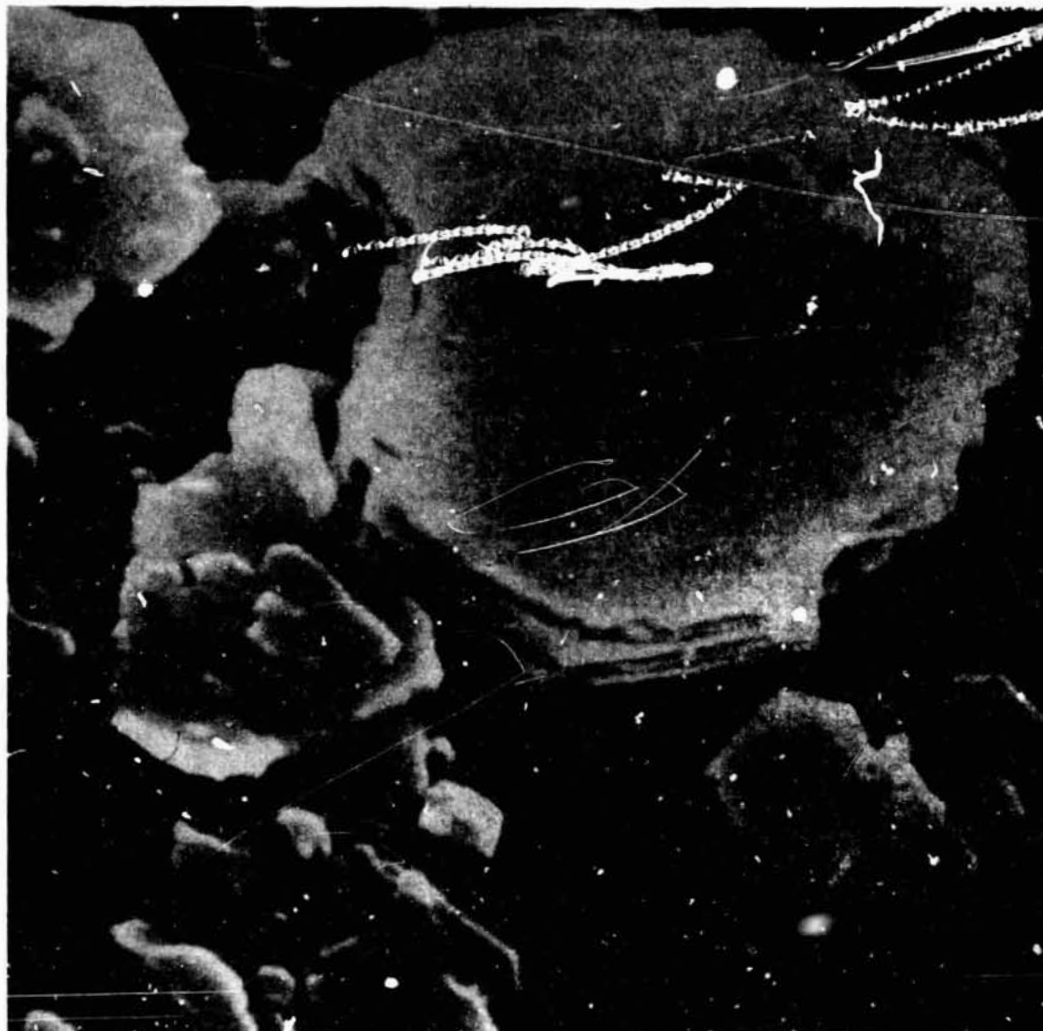
b) LV Sensitivity Function



c) Measurement Probability Distribution

ELECTRON MICROSCOPE PHOTOGRAPH OF KAOLIN PARTICLES

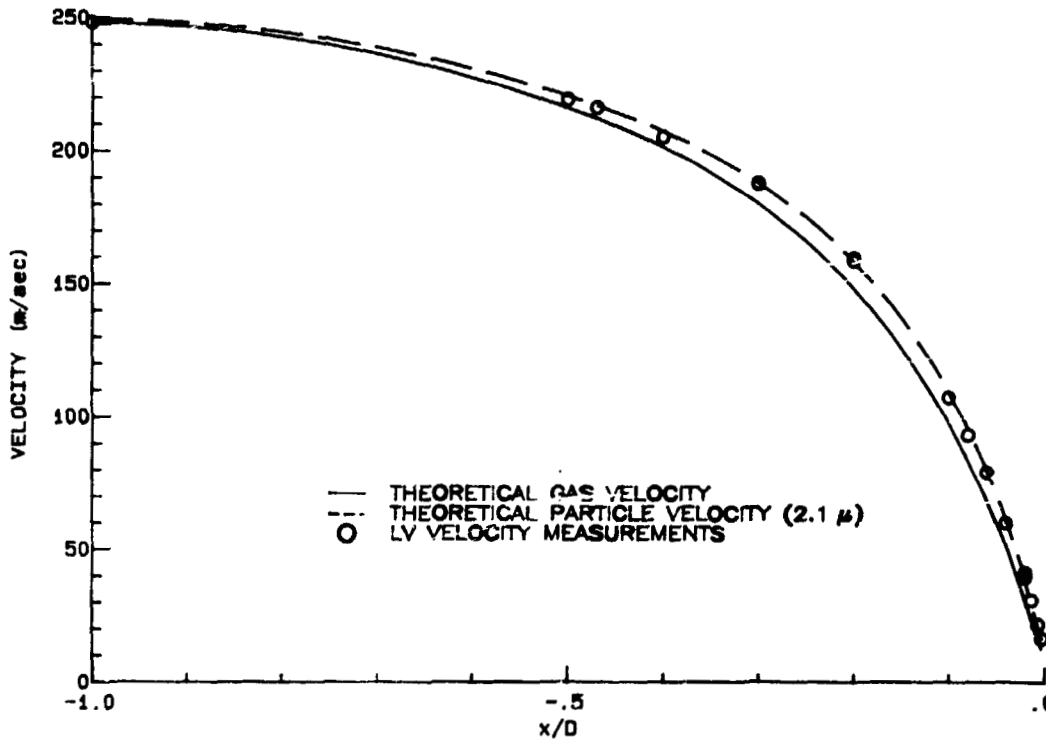
The irregular shapes and various sizes of the kaolin particles are shown in the electron microscope photograph.



ORIGINAL PRINT IS
OF POOR QUALITY

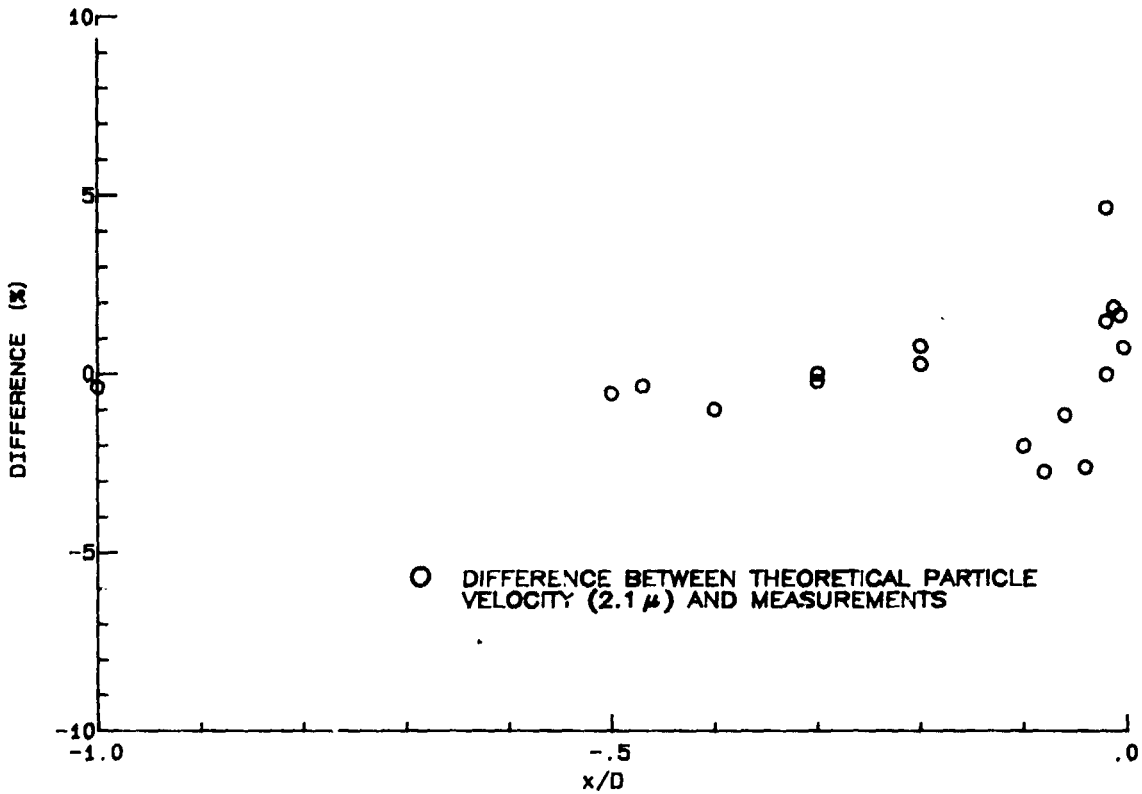
MEASUREMENTS ALONG THE STAGNATING STREAMLINE - MACH 0.8

The velocity measurements using kaolin along the stagnating streamline of the hemisphere-cylinder model at a tunnel setting of Mach 0.8 are presented in the figure along with the predicted gas velocity. The particle dynamic prediction procedures were used to determine that particles of 2.1 micrometers in diameter were the average kaolin particle size detected by the laser velocimeter.



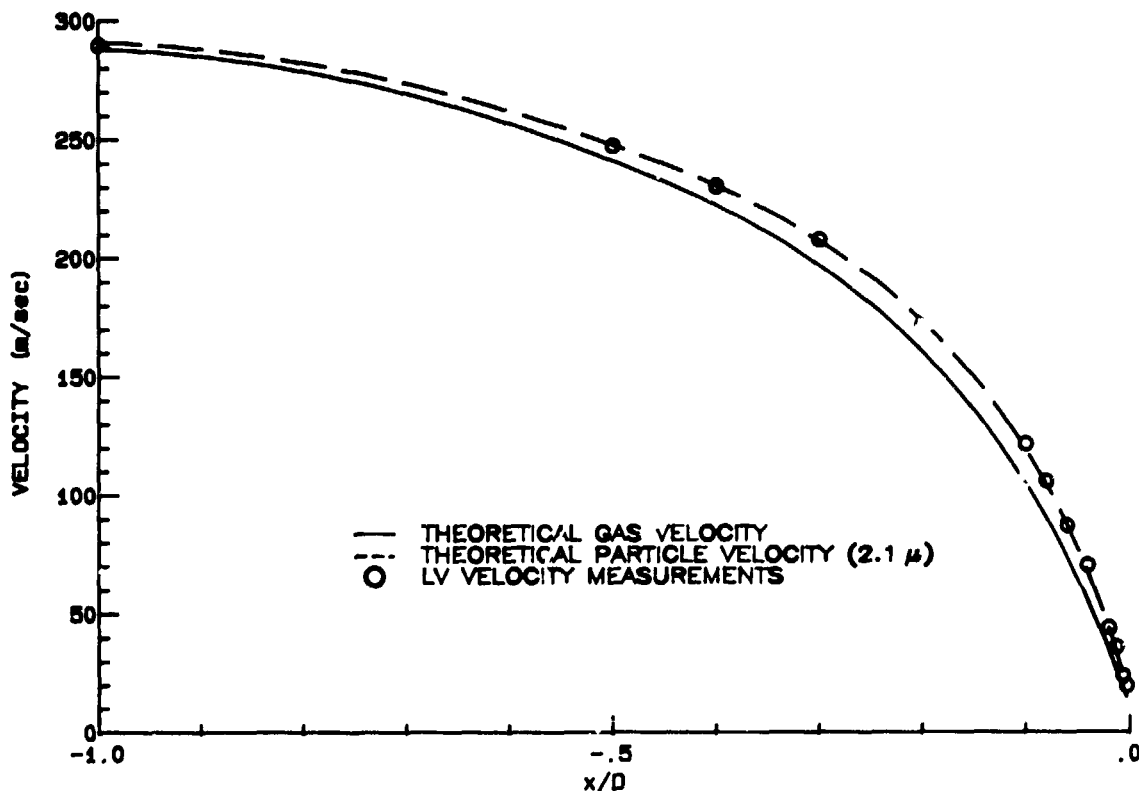
DIFFERENCES BETWEEN PARTICLE DYNAMIC THEORY AND MEASUREMENTS

The differences between the measured velocities and the predicted velocities for a 2.1 micrometer diameter kaolin are illustrated in the figure as a function of distance along the stagnating streamline of the hemisphere-cylinder model at Mach 0.8.



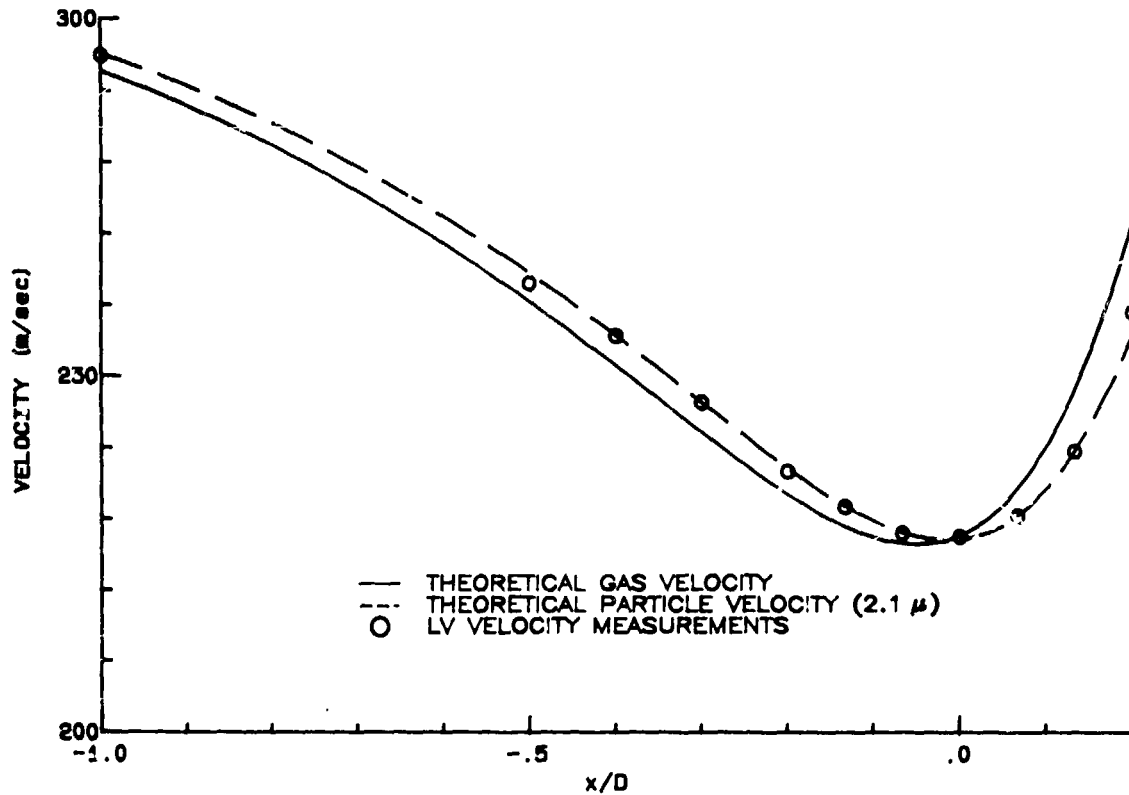
MEASUREMENTS ALONG THE STAGNATING STREAMLINE - MACH 1.0

The velocity measurements using kaolin along the stagnating streamline of the hemisphere-cylinder model at a tunnel setting of Mach 1.0 are presented in the figure along with the predicted gas velocity. The particle dynamic prediction procedures were used to determine that particles of 2.1 micrometers in diameter were the average kaolin particle size detected by the laser velocimeter.



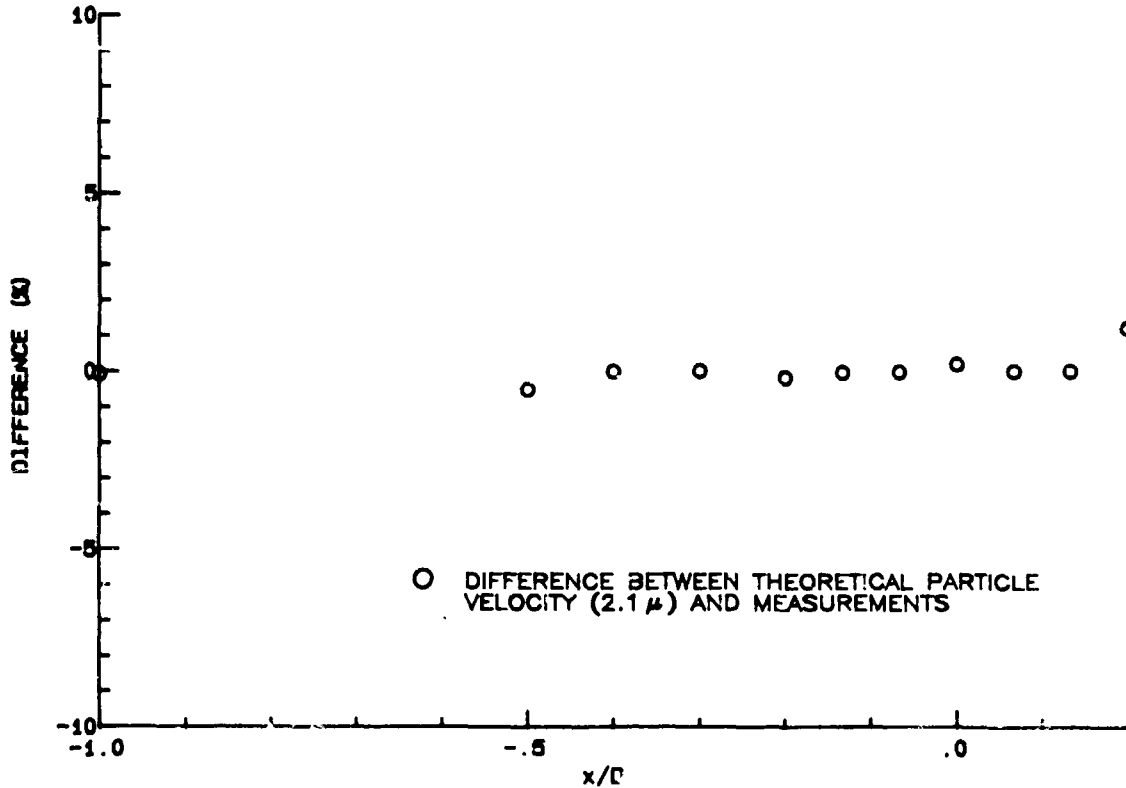
DIFFERENCES BETWEEN PARTICLE DYNAMIC THEORY AND MEASUREMENTS

The differences between the measured velocities and the predicted velocities for a 2.1 micrometer diameter kaolin are illustrated in the figure as a function of distance along the stagnating streamline of the hemisphere-cylinder model at Mach 1.0.



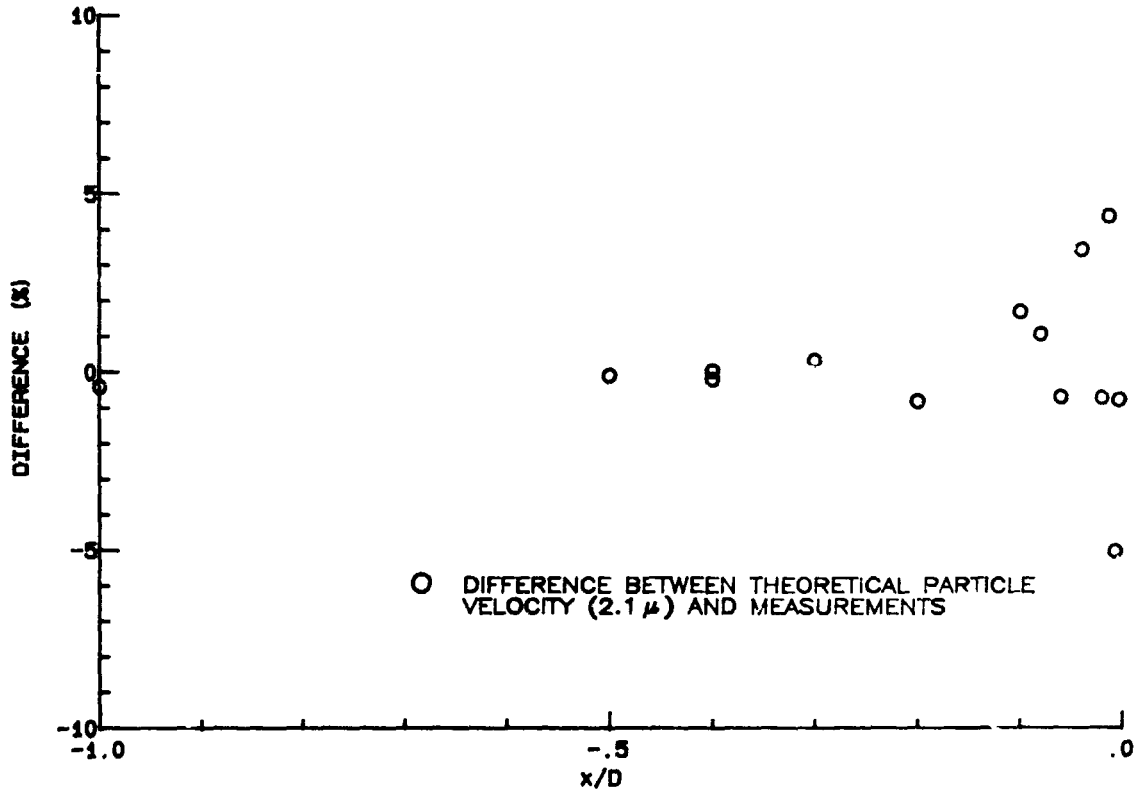
MEASUREMENTS ALONG $y/D = -0.533$ AT MACH 1.0

The velocity measurements using kaolin along a line 0.533 model diameters below the stagnating streamline of the hemisphere-cylinder model at a tunnel setting of Mach 1.0 are presented in the figure along with the predicted gas velocity. The particle dynamic prediction procedures were used to determine that particles of 2.1 micrometers in diameter were the average kaolin particle size detected by the laser velocimeter.



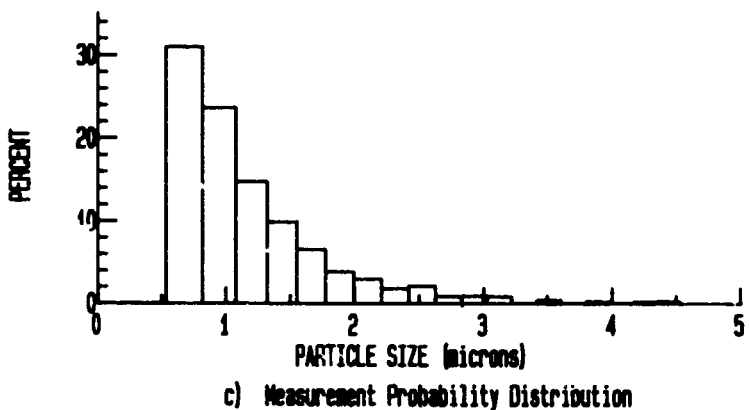
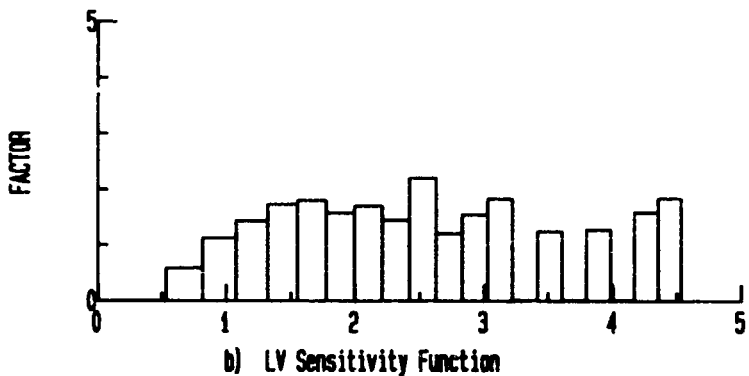
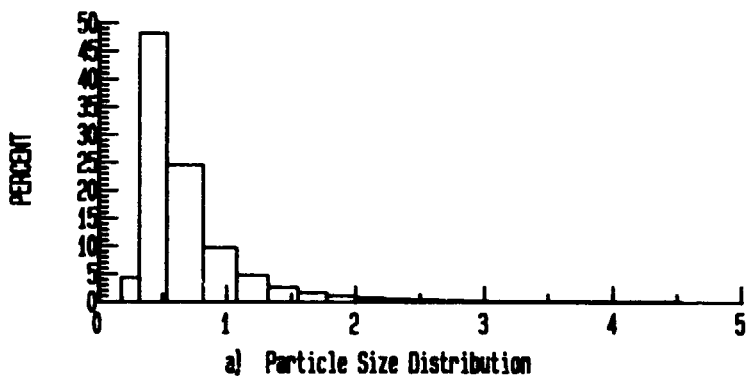
DIFFERENCES BETWEEN PARTICLE DYNAMIC THEORY AND MEASUREMENTS

The differences between the measured velocities and the predicted velocities for a 2.1 micrometer diameter kaolin are illustrated in the figure as a function of distance along the line 0.533 model diameters below the stagnating streamline of the hemisphere-cylinder model at Mach 1.0.



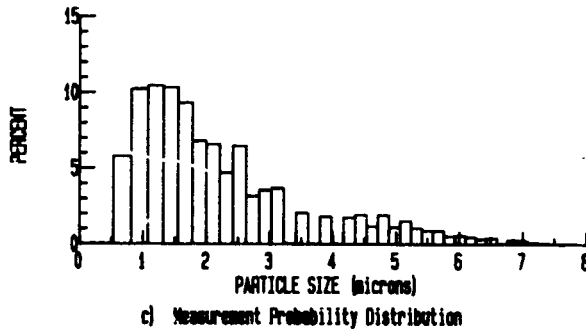
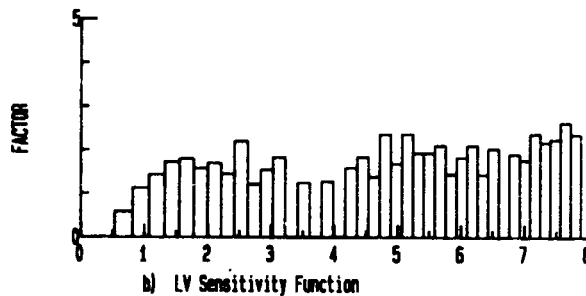
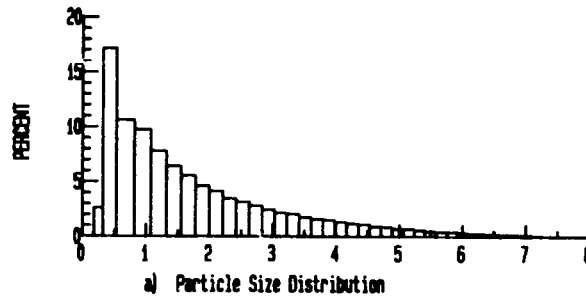
AERODYNAMIC PARTICLE SIZE ANALYSIS - KAOLIN

The particle size distribution measured with the aerodynamic particle size analyzer, laser velocimeter sensitivity function, and resulting particle size distribution of detectable particles for kaolin shown previously have been recalculated using the histogram widths for the optical particle size analyzer and are presented in the figure.



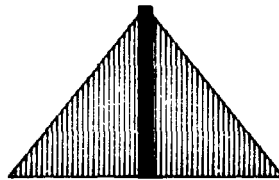
OPTICAL PARTICLE SIZE ANALYSIS - KAOLIN

Since the analysis of the predicted particle size distribution detectable by the laser velocimeter yielded an average particle of 0.78 micrometers in diameter and the velocity measurements obtained in the wind tunnel yielded an average particle of 2.1 micrometers in diameter, an optical particle size analyzer was used to remeasure the particle size distribution in the laboratory to determine the effect of the irregularly shaped particles on scattered light. The resulting measured distribution and the appropriate sensitivity function were combined to yield the detectable particle size distribution which had an average detectable particle size of 2.33 micrometers in diameter. Therefore the same particles have a different equivalent optical size from their equivalent aerodynamic size. This is most likely due to the greater optical effect from the random orientation of the irregularly shaped particles. Since the calculation of the laser velocimeter sensitivity function assumes a spherical particle, the effect of the irregularly shaped particles on the sensitivity of laser velocimeter cannot be predicted.

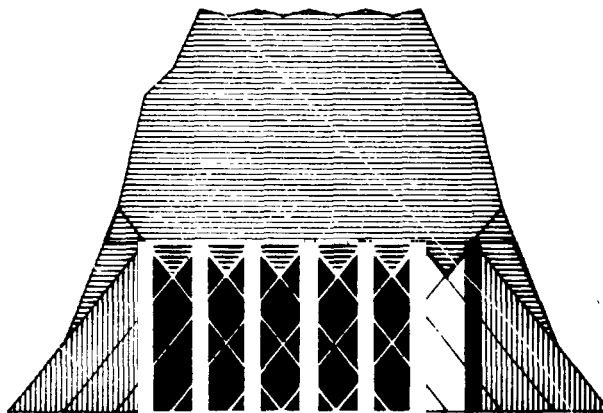


EFFECT OF PARTICLE DISTRIBUTION ON VELOCITY

As an aid in understanding the aerodynamic process involved in the present situation, consider the effect on the laser velocimeter measurements of the polydisperse particle distribution within the decelerating flow field as a combination of effects from each particle size. If the probability density function of the gas velocity at a location in the decelerating region is represented by the top figure, a uniformly polydisperse particle size distribution (e.g., seven particle sizes) within the flow would result in the probability density function given in the lower figure. By considering the polydisperse particle size distribution as being made up of individual particles, one finds that a zero diameter particle (i.e., the gas) would be found on the left or lowest velocity side of the distribution in the lower figure. As the particle size is increased, the resulting lag would shift its velocity distribution to the right of the lower figure. Therefore the resulting probability density function of particle velocity would be determined by a convolution of the probability density function of the gas velocity with the particle velocity lag characteristics as a function of particle size. From the lower figure it is found that a uniform particle size distribution results in a velocity distribution function which is approximately flat in the center. Therefore the measured velocity histograms in the decelerating regions may be used to estimate the particle size distribution measured by the laser velocimeter.



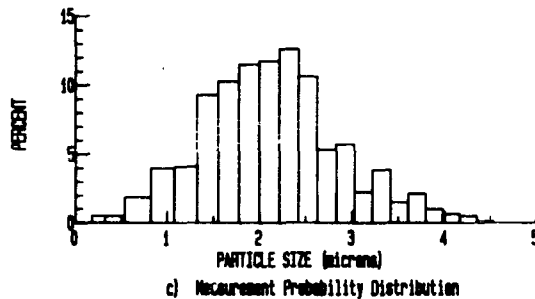
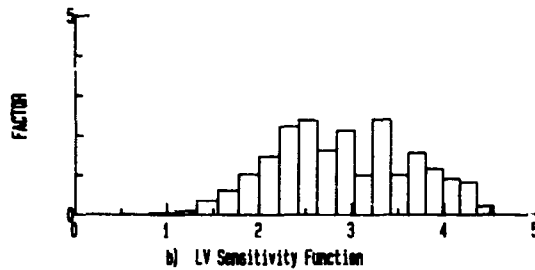
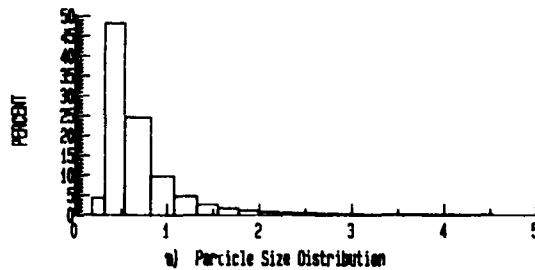
VELOCITY DISTRIBUTION



MEASURED HISTOGRAM

LV MEASUREMENT DERIVED PARTICLE SIZE - KAOLIN

At x/D distances of -0.4 and -0.5 the particle dynamic predictions indicate that the spread in velocity due to particle lag would be sufficient to segregate particle size provided the turbulence intensity of the flow was low. The measurements at these locations at Mach 1.0 indicated a "turbulence intensity" of 2 percent (including the spread due to particle lag). Assuming the velocities within the measured histograms below the predicted gas velocity were due to turbulence, the center portion of the histogram may be isolated by removing these velocities along with the corresponding high velocities (assuming symmetry). Each velocity within the clipped histogram was equated to a particle size based on the particle dynamic predictions to yield the detected particle size distribution. By dividing this distribution by the distribution obtained by the aerodynamic particle size analyzer, the laser velocimeter sensitivity function may be determined. It may be seen from the figure that the resulting sensitivity function approximates the previous sensitivity functions with the differences at the edges due to statistical uncertainty. The average detectable particle for this distribution was found to be 2.1 micrometers in diameter.



SEEDING RECOMMENDATIONS

The conclusion to be drawn from this investigation is that solid particles with a symmetric and narrow distribution should be used in laser velocimeter applications in high speed flows. Solid particles maintain their size distributions within the flow while liquids may be modified. A symmetric narrow distribution is needed to minimize the spread in velocity within regions containing velocity gradients thus increasing the accuracy of turbulence intensity measurements. The specific gravity of the material should be low but it should have a high index of refraction. The material which best fits these requirements is polystyrene.

- SOLID PARTICLES
- DENSITY SHOULD BE LOW
- INDEX OF REFRACTION SHOULD BE HIGH
- DISTRIBUTION SHOULD BE NARROW
- DISTRIBUTION SHOULD BE SYMMETRIC

IDEAL PARTICLE -> POLYSTYRENE

DENSITY - 1 gm/cc

INDEX OF REFRACTION - 1.56

TYPICAL STANDARD DEVIATION < 0.1 μ

REFERENCES

1. Meyers, J.F., and Walsh, M.J.: "Computer Simulation of a Fringe Type Laser Velocimeter," Proceedings of Project Squid Workshop on the Use of the Laser Velocimeter for Flow Measurements, Purdue University, March 27-29, 1974.
2. Mie, G.: "Optics of Turbid Media," Ann. Phys., vol. 25, no. 3, 1908, pp. 377-445.
3. Adrian, R.J., and Earley, W.L.: "Evaluation of LDV Performance Using Mie Scattering Theory," Presented at the Symposium on Laser Anemometry, University of Minnesota, October 22-24, 1975.
4. Reyhner, T.A.: "Computation of Transonic Potential Flow About Three Dimensional Inlets, Ducts, and Bodies," NASA CR-3514, 1982.
5. Walsh, M.J.: "Influence of Particle Drag Coefficient on Particle Motion in High-Speed Flow with Typical Laser Velocimeter Applications," NASA TN D-8120, 1976.